Journal of Thermal Analysis, Vol. 53 (1998) 389-396

Dedicated to Professor Ferenc Paulik on the occasion of his 75th birthday

KINETIC ANALYSIS OF SOLID STATE REACTIONS BY MEANS OF STEPWISE ISOTHERMAL ANALYSIS (SIA) AND CONSTANT RATE THERMAL ANALYSIS (CRTA)
A comparative study

F. J. Gotor, L. A. Perez-Maqueda, A. Ortega and J. M. Criado

Instituto de Ciencia de Materiales, Centro Mixto Universidad de Sevilla, C.S.I.C.,
Avda. Américo Vespucio s/n, 41092 Sevilla, Spain

Abstract

The results obtained in this work point out that both SIA and CRTA traces, simulated assuming the same values of the reaction rate, are identical provided that either '*n* order' or diffusion controlled kinetics are concerned. The α-T CRTA plots of solid state reactions fitting an Avrami-Erofeev kinetic model show that the temperature decreases with increasing α until reaching a minimum at a value of the reacted fraction $\alpha = \alpha_{min}$ characteristic of the Avrami-Erofeev exponent. The shapes of the corresponding SIA diagrams are quite different and a very long isothermal step is obtained. Moreover, the reaction rate is not maintained constant during the isothermal period but it shows a maximum at a value of α depending on the Avrami-Erofeev coefficient. It is important to point out that this α_{max} value agrees with the corresponding α_{min} calculated from a CRTA curve by assuming the same Avrami-Erofeev exponent.

Keywords: Constant Rate Thermal Analysis (CRTA), solid state kinetics, Stepwise Isothermal Analysis (SIA)

Introduction

Most thermal methods are still based on either isothermal or linear temperature programmes [1]. However, the methods based on the use of the own rate of reaction for controlling the reaction temperature seem to have some advantages over conventional approaches. Thus, it has been claimed that these methods would allow reducing the influence of heat and mass transfer phenomena on the forward solid state reactions in comparison with conventional thermal methods [2–4]. Moreover, it has been shown that these methods permit a more accurate determination of the kinetic model fitted for solid state reactions than conventional non-isothermal techniques [5–9]. These facts explain the relatively recent

1418–2874/98/ $ 5.00

Akadémiai Kiadó, Budapest
Kluwer Academic Publishers, Dordrecht

commercialization of the above methods by a number of manufacturers of thermobalances and dilatometers [10], including Netzsch, Setaram, TA Instruments, etc. Reading [11] has coined the term 'Constrained Rate Thermal Methods' for designing the different procedures that use the reaction rate for controlling the reaction temperature. The two best known methods are Constant Rate Thermal Analysis (CRTA) [12–22] and Stepwise Isothermal Analysis (SIA) [23–27]. Satoh and Hirota have used the SIA method for kinetic analysis of solid state reactions using an NMR signal for controlling the reaction rate [28]. Recently, TA Instruments has introduced in the market the technique of 'High Resolution Thermogravimetry', where the heating rate has a continuous sigmoidal relationship with the rate of mass change [11, 12]. Some methods for performing the kinetic analysis of data obtained from this technique have been developed in the literature [11, 29].

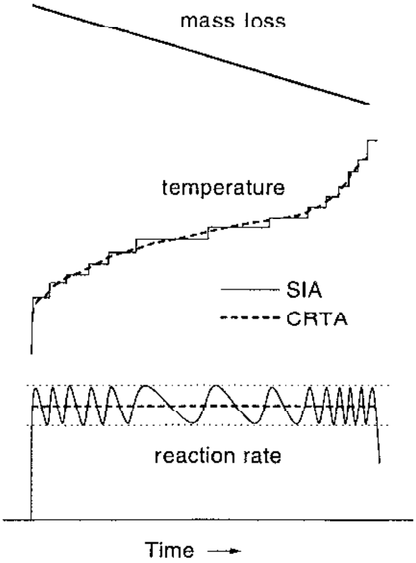

Fig. 1 A conventional comparison of SIA and CRTA curves obtained under similar conditions

CRTA and SIA are the most popular 'Constrained Rate Thermal Methods'. CRTA, independently developed by Rouquerol [12] and Paulik [13], implies a control of the temperature of the sample in such a way that the reaction rate remains constant at a pre-set value *C*. In Stepwise Isothermal Analysis (SIA), developed by Sørensen [23], the sample is heated at a constant rate until the reaction rate exceeds a pre-set limit, *C*. At this point the increase of temperature stops and the reaction proceeds isothermally until the rate becomes smaller than a lower limit, $C-\delta$, when the heating is resumed. The SIA temperature programme oscillates then between isothermal and rising temperature sections. In general, it seems to be assumed (provided that both the CRTA and SIA experiments are run by selecting the same reaction rate for controlling the reaction temperature) that the SIA trace approximately overlaps the corresponding CRTA plot as Fig. 1 shows.

However, it is worth pointing out the important difference between SIA and CRTA. SIA does not control the experiment if the rate becomes greater than the higher limit C. Thus, SIA would maintain an isothermal run and would allow the reaction rate to have any rate greater than the higher limit C for processes controlled by nucleation and growth of nuclei. This is because the reaction rate at a constant temperature increases with increasing α. The control would begin only after the rate decreases to the lower limit $C-\delta$. Studies of the shapes of SIA and CRTA curves depending on the kinetic model fitted for solid state reactions are still missing. The scope of this paper is to carry out this analysis and to test it in an experimental way.

Experimental

$Ni(NO)_3 \cdot 6H_2O$ Panreac a.r. was used. The anhydrous salt was prepared by dehydrating the corresponding hexahydrate in situ at 150°C.

A Cahn electrobalance, model 2000, attached to a high vacuum system was used. In order to perform CRTA experiments, the apparatus was modified for monitoring the furnace temperature in such a way that the total decomposition rate remains constant over the entire decomposition range. This was attained both by controlling the residual pressure in the close vicinity of the sample, by means of a PID controller, and by maintaining a constant value of the pumping rate, which can be selected by means of a valve. The control of the temperature during the SIA experiment was carried out using a linear heating programmer interfaced to an ON/OFF controller that monitors the partial pressure of the gases self-generated in the reaction. Thus, the sample temperature was increased at a constant rate until the pressure exceeded the pre-set value, at which point the temperature was maintained constant until the pressure became smaller than the limit, when the increase of temperature was resumed.

The CRTA and SIA curves were recorded using a residual pressure of 10^{-4} mbar and a decomposition rate of $2.5 \cdot 10^{-3}$ min^{-1}. The SIA experiment was started at a heating rate $\beta=4$ K min^{-1}. The starting sample mass was about 25 mg of anhydrous nickel nitrate.

Simulation of CRTA and SIA curves

If the reaction rate is maintained constant at a value C, we can write

$$\frac{d\alpha}{dt} = C = A e^{-E/RT} f(\alpha) \qquad (1)$$

Theoretical CRTA curves can be obtained from Eq. (1) for given values of the preexponential factor of Arrhenius, A, and the activation energy, E.

SIA curves were calculated by simulating the α–T trace at the previously selected heating rate until reaching the pre-set value of the reaction rate, C. The temperature reached at this point is maintained constant until the rate becomes smaller than $C-\delta$ when it is assumed that the temperature increases again at a heating rate of β.

This process is repeated until the α–t (or T) curve is completed. The constant heating rate steps were calculated from the following equation:

$$g(\alpha) - g(\alpha_o) = \int_{\alpha_o}^{\alpha} \frac{\mathrm{d}\alpha}{f(\alpha)} = \frac{A}{\beta}\int_{T_o}^{T} e^{-E/RT} \tag{2}$$

The integration of the Arrhenius equation was performed by means of a computer by numerical methods. The isothermal parts of the SIA curve were calculated from the expression:

$$g(\alpha) = \int_{\alpha_o}^{\alpha} \frac{\mathrm{d}\alpha}{f(\alpha)} = k_T(t - t_o) \tag{3}$$

where k_T is the constant rate at temperature T, t_o is the time at which the isothermal section starts and t is the time at which the reacted fraction is equal to α.

Figure 2 shows the CRTA plots calculated at a constant reaction rate $C=2.10^{-2}$ min^{-1} for a reaction obeying an R_3 kinetic model with the following kinetic parameters: $A=10^8$ min^{-1} and $E=160$ kJ mol^{-1}. The corresponding SIA curve calculated assuming the same kinetic parameters, a reaction rate $C \cong C-\delta=2.10^{-2}$ min^{-1} and a starting heating rate $\beta=10$ K min^{-1} was also included in Fig. 2. It is shown that the SIA trace starts with a conventional linear heating curve until the reaction rate reaches the pre-set value C. From this point, the temperature is controlled by the reaction rate and the SIA curve overlaps the CRTA curve, provided that the two limits of reaction rates at which the increase of temperature stops (C) and the one at which the increase of temperature is resumed again ($C-\delta$) are close enough. As the δ band is broadened the second part of the SIA trace becomes a set of isothermal steps as represented in Fig. 1. The same agreement between SIA and CRTA traces was obtained considering either an R_2 kinetic model or diffusion models (D_2, D_3, D_4).

Figure 3 shows the CRTA plot calculated by using the same constant reaction rate, C, and kinetic parameters identical to those used in Fig. 2 but assuming an A_2 Avrami-Erofeev kinetic model. It can be observed that, once the reaction rate reaches the pre-set value C, the temperature decreases until the reacted fraction

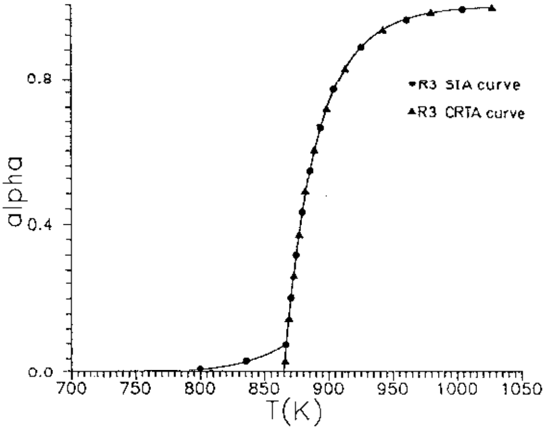

Fig. 2 CRTA and SIA plots calculated for an R_3 kinetic model assuming the following kinetic parameters: E=160 kJ mol^{-1}, A=10^{8} min^{-1}. CRTA (C=2.10^{-2} min^{-1}); SIA (β=10°K min^{-1} and C=2·10^{-2} min^{-1})

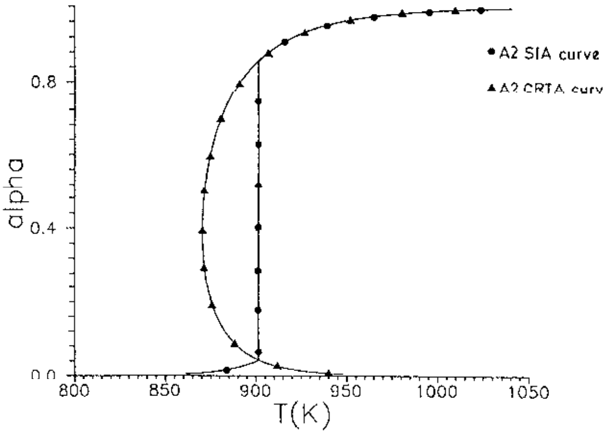

Fig. 3 CRTA and SIA curves calculated for an A_2 kinetic model assuming the same conditions and kinetic parameters as used in Fig. 2

reaches a value α_{min} that corresponds to a minimum in the T–α plot (i.e., $d^2T/d\alpha^2 = 0$). The values of α_{min} as a function of the Avrami-Erofeev exponent have been reported in a previous paper [22]. It is worth pointing out that the temperature cannot decrease under SIA control but an isothermal section is maintained until the reaction rate decreases again below the pre-set value. The SIA curve simulated for an A_2 kinetic model by assuming a starting heating rate β=10 K min^{-1} and the same kinetic parameters as used previously for simulating the corresponding CRTA trace is also shown in Fig. 3. It can be observed that the

SIA curve becomes like an isothermal curve in almost the whole α range as previously forecast.

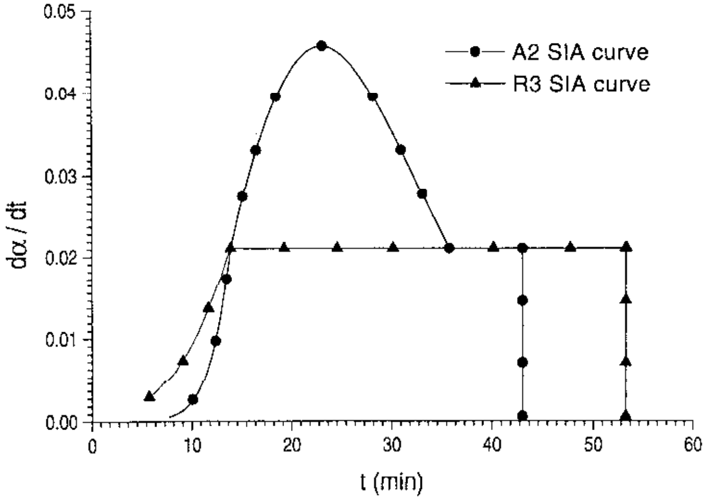

Fig. 4 Plot of $\mathrm{d}\alpha/\mathrm{d}t$ as a function of the time corresponding to the SIA curves included in Figs 2 and 3

In order to summarize the above results it may be illustrative to compare the plots of the $\mathrm{d}\alpha/\mathrm{d}t$ values of the SIA curves included in Figs 2 and 3 as a function of the time. These plots are shown in Fig. 4. It is observed that for the R_3 model the reaction rate remains constant once the pre-set value C is reached. Similar results would be obtained from SIA traces corresponding to either R_2 or diffusion (D_2, D_3, D_4) kinetic models. However, reactions fitting an Avrami-Erofeev kinetic law are not characterized by a constant value of $\mathrm{d}\alpha/\mathrm{d}t$ but the SIA control leads to an isothermal section and, consequently, to a $\mathrm{d}\alpha/\mathrm{d}t$–$t$ plot with a mathematical maximum. If we take into account that the rate of a reaction obeying an Avrami-Erofeev kinetics can be represented under isothermal conditions by the following equation:

$$\frac{\mathrm{d}\alpha}{\mathrm{d}t}=n(1-\alpha)[-\ln(1-\alpha)]^{1-1/n} \tag{4}$$

n being the Avrami-Erofeev exponent, and that at the maximum $\mathrm{d}^2\alpha/\mathrm{d}t^2=0$, we get:

$$\ln\frac{1}{1-\alpha_{\max}}=1-\frac{1}{n} \tag{5}$$

Table 1 Values of α_{max} calculated according to Eq. (5) for Avrami-Erofeev kinetic models with $n>1$

n	2.0	3.0	4.0
α_{max}	0.393	0.487	0.528

The values of α_{max} calculated according to Eq. (5) for Avrami-Erofeev kinetic models with $n>1$ are shown in Table 1. It is to be pointed out that these α_{max} values agree with the corresponding α_{min} values calculated from CRTA curves by assuming the same n value.

Results

In order to check experimentally the above conclusions, the CRTA curve shown in Fig. 5 was obtained for the thermal decomposition of anhydrous nickel nitrate. It has been stated earlier [30] based on TG data combined with the results of mass spectrometry experiments that the thermal decomposition of nickel nitrate takes place in a single step, represented by the equation

$$Ni(NO_3)_2 \rightarrow NiO + 2NO_2 + 1/2O_2 \qquad (6)$$

It has also been concluded [30] that this transformation obeys the Avrami-Erofeev kinetic law with an exponent $n=2$. This results has been interpreted by a reaction mechanism that involves instantaneous nucleation on the surface of the crystal with subsequent growth of the nuclei into particles. The shape of the α *vs.* T plot in Fig. 5 is highly characteristic of an Avrami-Erofeev model [22]. On the

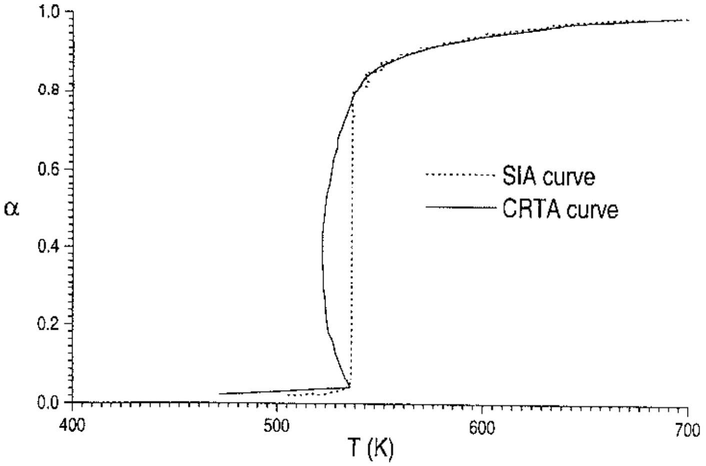

Fig. 5 SIA and CRTA curves recorded for the thermal decomposition of anhydrous nickel nitrate under the conditions described in the experimental part

other hand, it is also shown in Fig. 5 that the SIA curve obtained for the thermal decomposition of this compound becomes isothermal once the decomposition rate achieves the pre-set value, *C*, which agrees quite well with our previous forecasting.

References

1 M. Reading, '6th European Symposium on Thermal Analysis and Calorimetry' (ESTAC 6), Book of Abstract, Grado (Italy), 1994, p. 246.
2 J. M. Criado, F. Rouquerol and J. Rouquerol, Thermochim. Acta, 38 (1980) 109.
3 A. Ortega, S. Akhowyasi, F. Rouquerol and J. Rouquerol, Thermochim. Acta, 38 (1980) 109.
4 L. A. Perez-Maqueda, A. Ortega and J. M. Criado, Thermochim. Acta, 277 (1996) 165.
5 J. M. Criado, F. Rouquerol and J. Rouquerol, Thermochim. Acta, 38 (1980) 117.
6 J. M. Criado, A. Ortega, J. Rouquerol and F. Rouquerol, Thermochim. Acta, 240 (1994) 247.
7 J. M. Criado, L. A. Perez-Maqueda and A. Ortega, J. Thermal Anal., 42 (1994) 551.
8 A. Ortega, L. A. Perez-Maqueda and J. M. Criado, Thermochim. Acta, 282/283 (1996) 29.
9 A. Ortega, Thermochim. Acta, 298 (1997) 205.
10 P. S. Gill, R. S. Sauerbrunn and B. S. Crowe, J. Thermal Anal., 38 (1992) 255.
11 M. Reading, Controlled Rate Thermal analysis and beyond, in E. L. Charsley and S. B. Warrington (Eds.), Thermal Analysis-Techniques & Applications, The Royal Society of Chemistry, London 1992.
12 J. Rouquerol, Bull. Soc. Chim., (1964) 31.
13 F. Paulik and J. Paulik, Anal. Chim. Acta, 56 (1971) 328.
14 J. Paulik and F. Paulik, Simultaneous Thermoanalytical examination by means of the derivatograph, in series Wilson-Wilson's Comprehensive Analytical Chemistry, Vol. XII, Elevier, Amsterdam 1981.
15 M. H. Stacey, Anal. Proc., 22 (1985) 242.
16 J. Paulik, F. Paulik and M. Arnold, J. Thermal Anal., 32 (1987) 301.
17 F. Paulik, S. Gal and K. M. Szécsenyi, J. Thermal Anal., 42 (1994) 425.
18 G. Thevand, F. Rouquerol and J. Rouquerol, Material Science Monographs, 28 B (1985) 727.
19 F. Rouquerol, Y. Laureiro and J. Rouquerol, Solid State Ionics, 63 (1993) 164.
20 N. Koga, J. M. Criado and H. Tanaka, J. Thermal Anal., 49 (1997) 1467.
21 J. M. Criado, Thermochim. Acta, 28 (1979) 307.
22 J. M. Criado, M. D. Alcalá and C. Real, Solid State Ionics, 101–103 (1997) 1387.
23 O. T. Sørensen, J. Thermal Anal., 13 (1978) 429.
24 O. T. Sørensen, Thermochim. Acta, 50 (1981) 163.
25 O. T. Sørensen, Thermochim. Acta, 85 (1985) 287.
26 P. L. Husum and O. T. Sørensen, Thermochim. Acta, 114 (1987) 131.
27 O. T. Sørensen, J. Thermal Anal., 38 (1992) 213.
28 M. Satoh and M. Hirota, Nippon Kagaku Kaishi, (1996) 341.
29 I. Salin and J. C. Seferis, J. Applied Polymer Si., 47 (1993) 847.
30 J. M. Criado, A. Ortega and C. Real, React. Solids, 4 (1987) 93.